

## Equation of State and Critical Point of Cesium

N. B. Vargaftik,<sup>1</sup> E. B. Gelman,<sup>2</sup> V. F. Kozhevnikov,<sup>1</sup> and S. P. Naursakov<sup>2</sup>

*Received April 25, 1989*

---

Equation-of-state measurements for cesium at temperatures from 350 to 2200 K and pressures from 1 to 60 MPa by means of a hermetically sealed two-zone dilatometer are presented. The experimental range includes the liquid and gaseous phases together with the coexistence curve up to critical point and supercritical region. The critical parameters are 1938 K, 9.4 MPa, 0.39 g · cm<sup>-3</sup>. The data were used for the calculation of tables of the density and its derivatives for cesium. The results are discussed.

---

**KEY WORDS:** cesium; compressibility; critical parameters; density; dilatometer; equation of state; high temperatures; thermal expansion.

### 1. INTRODUCTION

Cesium and other alkali metals are simple metals. The fermi surface of these metals is spherical [1]. Hence, to understand distinctions between physical properties of metallic those of and nonmetallic liquids (especially at low density), it is necessary to study some of them in detail. The equations-of-state data are of paramount importance for this problem, since they are necessary for the interpretation of the data on other properties. Therefore, it is no coincidence that high-temperature equations-of-state data of cesium were obtained in a comparatively large number of investigations [2]. However, the precision of most of them is insufficient for the *PVT* properties of cesium at high temperatures.

In this work (which is a continuation of earlier studies [3, 4]) the equation of state of cesium is studied not only in the liquid phase, but also in the gaseous phase, including coexistence curve. It permits us to exclude errors of extrapolation of experimental isobars to the saturation state, to

---

<sup>1</sup> Moscow Aviation Institute, Moscow 125871, USSR.

<sup>2</sup> Kurchatov Institute of Atomic Energy, Moscow 123182, USSR.

calculate *PVT* properties of cesium fluid (density and its derivatives), to obtain reliable values of the critical parameters, and to reveal some anomalies peculiarities of the equation of state of cesium near the critical point.

In Section 2, a brief description of the experimental procedure, estimate of errors and results of measurements are given. A local smoothing of the experimental data and the *PVT* properties of cesium are considered in Section 3. The results are discussed in Section 4.

## 2. EXPERIMENTAL

The experimental apparatus has been described in the literature [5] in detail. In the present work, the stainless cylindrical membrane [5] was replaced by a soft bellows of the same material. The improvement has permitted us to extend considerably the range of dilatometer-volume

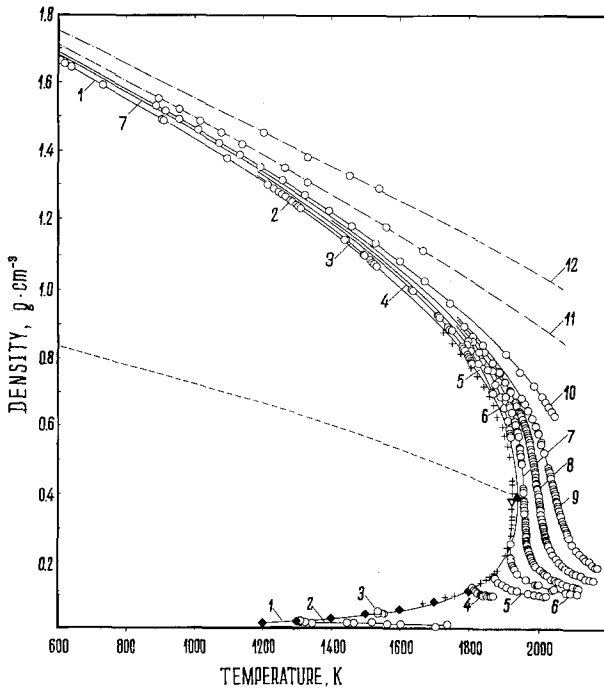


Fig. 1. Cesium equation of state (experimental data). 1, Saturation curve. Isobars: 2, 0.98 MPa; 3, 3.04 MPa; 4, 6.96 MPa; 5, 7.94 MPa; 6, 8.92 MPa; 7, 9.90 MPa; 8, 10.7 MPa; 9, 11.9 MPa; 10, 14.8 MPa; 11, 29.5 MPa; 12, 58.9 MPa. ▲—Critical point; ◆—vapor density of saturation [8]; +, ▽—experimental data and critical point [9].

variation  $\Delta V$ , when the pressure difference  $\Delta P$  between the inside and the outside of the dilatometer is negligible [6]. When  $\Delta V = 2.2 \text{ cm}^3$  the pressure difference  $\Delta P = 20 \text{ kPa}$ . The volume of the molybdenum and tungsten dilatometer cells was about  $1.7 \div 2.0 \text{ cm}^3$ . The capillary volume was  $\sim 10^{-2} V_{\text{cell}}$ .

The dilatometer, filled under high vacuum with cesium and the mercury as the intermediate liquid, was placed in a high-pressure vessel, separated into hot and cold zones. Argon was used as the pressurizing

Table I. Density of Cesium,  $\rho$ , in  $\text{g} \cdot \text{cm}^{-3}$

$T$ (K)	At saturation			$10^{-5} P$ (Pa)						
	$P_s^b$	$\rho_V^a$	$\rho_L^a$	50	90	100	200	300	400	600
400	0.0		1.781	1.787	1.792	1.794	1.806	1.818	1.830	1.854
500	0.0		1.723	1.730	1.736	1.738	1.752	1.765	1.778	1.804
600	0.0		1.666	1.674	1.680	1.682	1.697	1.712	1.726	1.754
700	0.1		1.609	1.617	1.624	1.626	1.643	1.659	1.675	1.704
800	0.2		1.552	1.561	1.569	1.571	1.588	1.605	1.622	1.654
900	0.7	0.001 <sup>a</sup>	1.494	1.505	1.513	1.515	1.533	1.552	1.570	1.604
1000	1.7	0.003 <sup>a</sup>	1.435	1.446	1.455	1.457	1.477	1.497	1.516	1.554
1050	2.5	0.004 <sup>a</sup>	1.404	1.416	1.425	1.427	1.448	1.469	1.490	1.529
1100	3.6	0.006 <sup>a</sup>	1.373	1.385	1.395	1.397	1.419	1.441	1.463	1.504
1150	5.1	0.008 <sup>a</sup>	1.341	1.353	1.364	1.366	1.390	1.413	1.436	1.479
1200	6.9	0.011 <sup>a</sup>	1.308	1.321	1.333	1.335	1.361	1.385	1.409	1.454
1250	9.1	0.014	1.274	1.287	1.301	1.304	1.331	1.357	1.382	1.429
1300	12	0.017	1.238	1.252	1.268	1.272	1.301	1.328	1.354	1.404
1350	15	0.021	1.201	1.216	1.234	1.238	1.271	1.300	1.327	1.379
1400	19	0.025	1.163	1.179	1.199	1.204	1.240	1.271	1.299	1.354
1450	23	0.030	1.124	1.141	1.163	1.168	1.208	1.241	1.272	1.330
1500	28	0.036	1.085	1.101	1.126	1.131	1.175	1.211	1.244	1.305
1550	33	0.043	1.043	1.057	1.086	1.093	1.142	1.181	1.216	1.280
1600	39	0.051	1.000	1.011	1.044	1.052	1.108	1.149	1.187	1.256
1650	45	0.060	0.955	0.960	1.001	1.011	1.072	1.118	1.158	1.231
1700	52	0.072	0.905	—	0.956	0.965	1.036	1.086	1.128	1.206
1750	60	0.090	0.850	—	0.904	0.915	0.998	1.053	1.097	1.180
1800	68	0.114	0.789	—	0.842	0.857	0.957	1.020	1.067	1.154
1850	76	0.147	0.717	—	0.766	0.790	0.918	0.987	1.035	1.127
1900	86	0.207	0.614	—	0.654	0.703	0.877	0.954	1.004	1.100
1950	—	—	—	—	—	0.533	0.834	0.921	0.972	1.073
2000	—	—	—	—	—	0.189	0.792	0.888	0.940	1.045
2050	—	—	—	—	—	0.149	0.747	0.856		
2100	—	—	—	—	—	0.132				

<sup>a</sup> Data of Ref. 8.

<sup>b</sup> Data of Ref. 7.

medium. Cesium, that was in the hermetical dilatometer volume, was pressurized by argon medium through piston, mercury and bellows.

The cell in the hot zone was heated by three tungsten resistance furnaces [4, 5]. The cell temperature in the hot zone was measured with three calibrated W-Re 5/20 thermocouples. The temperature gradients along the cell were  $\Delta T/T \leq 10^{-3}$ .

The standard error of the W-Re thermocouples increases from 5 K at 1300 K to 10 K at 2100 K. The pressure was measured with precision manometers with an error of 20 kPa for  $P \leq 10$  MPa and of 100 kPa for pressures  $p > 10$  MPa. The error of the density data varies from

**Table II.** Thermal Expansion of Cesium,  $10^3 \alpha_p$ , in  $K^{-1}$

$T$ (K)	At saturation		$10^{-5} P$ (Pa)							
	$P_s$	$(\alpha_p)_L^s$	50	90	100	200	300	400	500	600
400	0.0	0.32	0.32	0.31	0.31	0.30	0.29	0.29	0.28	0.27
500	0.0	0.33	0.32	0.32	0.32	0.31	0.30	0.30	0.29	0.28
600	0.0	0.34	0.33	0.33	0.33	0.32	0.31	0.30	0.29	0.29
700	0.1	0.35	0.34	0.34	0.34	0.33	0.32	0.31	0.30	0.29
800	0.2	0.37	0.36	0.36	0.35	0.34	0.33	0.32	0.31	0.30
900	0.7	0.39	0.38	0.37	0.37	0.36	0.34	0.33	0.32	0.31
1000	1.7	0.43	0.41	0.40	0.40	0.38	0.36	0.35	0.33	0.32
1050	2.5	0.45	0.43	0.42	0.41	0.39	0.37	0.35	0.33	0.33
1100	3.6	0.47	0.45	0.43	0.43	0.40	0.38	0.36	0.34	0.33
1150	5.1	0.50	0.47	0.45	0.45	0.41	0.39	0.37	0.35	0.34
1200	6.9	0.53	0.49	0.47	0.47	0.42	0.40	0.38	0.36	0.34
1250	9.1	0.57	0.52	0.49	0.49	0.44	0.41	0.38	0.36	0.35
1300	12	0.61	0.56	0.52	0.51	0.45	0.42	0.39	0.37	0.36
1350	15	0.66	0.59	0.55	0.54	0.47	0.43	0.40	0.38	0.36
1400	19	0.71	0.64	0.58	0.57	0.49	0.44	0.41	0.39	0.37
1450	23	0.76	0.69	0.61	0.60	0.51	0.45	0.42	0.40	0.38
1500	28	0.83	0.74	0.65	0.64	0.53	0.47	0.43	0.40	0.38
1550	33	0.91	0.82	0.70	0.68	0.57	0.49	0.44	0.41	0.39
1600	39	1.0	0.93	0.76	0.73	0.59	0.51	0.46	0.42	0.40
1650	45	1.1	1.1	0.88	0.82	0.62	0.53	0.48	0.44	0.41
1700	52	1.3	—	1.0	0.95	0.66	0.55	0.50	0.46	0.42
1750	60	1.6	—	1.3	1.2	0.72	0.58	0.52	0.48	0.44
1800	68	2.3	—	1.6	1.5	0.78	0.61	0.54	0.50	0.46
1850	76	3.6	—	2.4	1.9	0.86	0.64	0.57	0.52	0.48
1900	86	7.1	—	5.0	3.1	0.95	0.67	0.60	0.54	0.50
1950	—	—	—	—	18	1.1	0.71	0.63	0.57	0.52
2000	—	—	—	—	9.2	1.2	0.75	0.66	0.60	0.54
2050	—	—	—	—	3.7	1.4	0.80	—	—	—
2100	—	—	—	—	1.9	—	—	—	—	—

0.2% for the dense liquid ( $\rho \geq 1.5 \text{ g} \cdot \text{cm}^{-3}$ ) to 1% for the vapor ( $\rho \leq 2.10^{-2} \text{ g} \cdot \text{cm}^{-3}$ ).

The experimental data are shown in Fig. 1. The measurements were performed along isobars at stationary conditions under both increasing and decreasing sample temperature. The majority of the experimental points was obtained at pressures of 1, 3, 7, 8, 9, 10, 11, and 12 MPa. The data obtained at higher pressures agreed with our earlier data [4]. Therefore the number of new data at pressures  $p > 15 \text{ MPa}$  is not large. The data for isobars at 30 and 59 MPa, shown in Fig. 1, are given in Ref. 4.

The liquid-gas transition temperature  $T_s$  was determined from the density jump under heating and cooling of the sample. The error of these

Table III. Isothermal Compressibility of Cesium,  $10^9 k_T$ , in  $\text{Pa}^{-1}$

$T(\text{K})$	At saturation		$10^{-5} P (\text{Pa})$							
	$P_s$	$(k_T)_L^s$	50	90	100	200	300	400	500	600
400	0.0	0.74	0.73	0.72	0.72	0.71	0.69	0.67	0.65	0.63
500	0.0	0.86	0.84	0.83	0.83	0.80	0.77	0.75	0.72	0.70
600	0.0	0.99	0.96	0.94	0.94	0.90	0.86	0.83	0.80	0.78
700	0.1	1.1	1.1	1.1	1.1	1.0	0.98	0.94	0.90	0.87
800	0.2	1.3	1.3	1.2	1.2	1.2	1.1	1.1	1.0	0.97
900	0.7	1.5	1.5	1.4	1.4	1.3	1.3	1.2	1.1	1.1
1000	1.7	1.8	1.8	1.7	1.7	1.6	1.4	1.4	1.3	1.2
1050	2.5	2.0	1.9	1.9	1.8	1.7	1.6	1.5	1.4	1.3
1100	3.6	2.3	2.1	2.0	2.0	1.8	1.7	1.6	1.5	1.4
1150	5.1	2.5	2.4	2.2	2.2	2.0	1.8	1.7	1.6	1.5
1200	6.9	2.8	2.6	2.5	2.4	2.1	1.9	1.8	1.7	1.6
1250	9.1	3.2	2.9	2.7	2.7	2.3	2.1	1.9	1.8	1.7
1300	12	3.7	3.3	3.0	3.0	2.5	2.3	2.1	1.9	1.8
1350	15	4.2	3.8	3.4	3.3	2.8	2.5	2.2	2.0	1.9
1400	19	4.9	4.4	3.9	3.8	3.1	2.7	2.4	2.2	2.0
1450	23	5.7	5.1	4.4	4.3	3.4	3.0	2.6	2.3	2.1
1500	28	6.7	5.9	5.1	4.9	3.8	3.2	2.8	2.5	2.2
1550	33	8.0	7.2	5.9	5.6	4.3	3.5	3.1	2.7	2.4
1600	39	9.6	8.8	6.9	6.6	4.8	3.9	3.3	2.9	2.6
1650	45	12	11	8.4	7.9	5.4	4.3	3.7	3.2	2.8
1700	52	15	—	11	10	6.2	4.8	4.0	3.5	3.0
1750	59	23	—	15	13	7.3	5.4	4.6	3.8	3.3
1800	68	41	—	21	19	8.6	6.0	5.0	4.2	3.5
1850	76	78	—	34	29	10	6.7	5.5	4.6	3.9
1900	86	230	—	100	62	12	7.6	6.2	5.1	4.2
1950	—	—	—	—	500	15	8.6	6.9	5.6	4.6
2000	—	—	—	—	470	19	9.8	7.7	6.2	5.0
2050	—	—	—	—	350	24	11	—	—	—
2100	—	—	—	—	260	—	—	—	—	—

measurements was  $\leq 1$  K on the thermometer scale used. The measured values of the gas-liquid transition temperature at pressures up to 9 MPa were in agreement with earlier  $P_s - T_s$  data [7]. On the experimental isobars at pressures  $P \geq 10$  MPa boiling was not observed.

The points which correspond to the saturated vapor density [8] are also shown in Fig. 1. These are in a good agreement with our data at temperatures up to 1800 K. The critical parameters are as follows:

$$T_c = 1938 \pm 10 \text{ K}, \quad P_c = 9.4 \pm 0.2 \text{ MPa}, \quad \rho_c = 0.39 \pm 0.01 \text{ g} \cdot \text{cm}^{-3} \quad (1)$$

These parameters disagree with earlier data (see Ref. 2), but they agree with recent data reported by Jungst et al. [9] (see Fig. 1).

### 3. ANALYSIS OF EXPERIMENTAL DATA

For a calculation of the  $PVT$  properties the experimental data need to be smoothed. Obviously, the results will depend on the smoothing method.

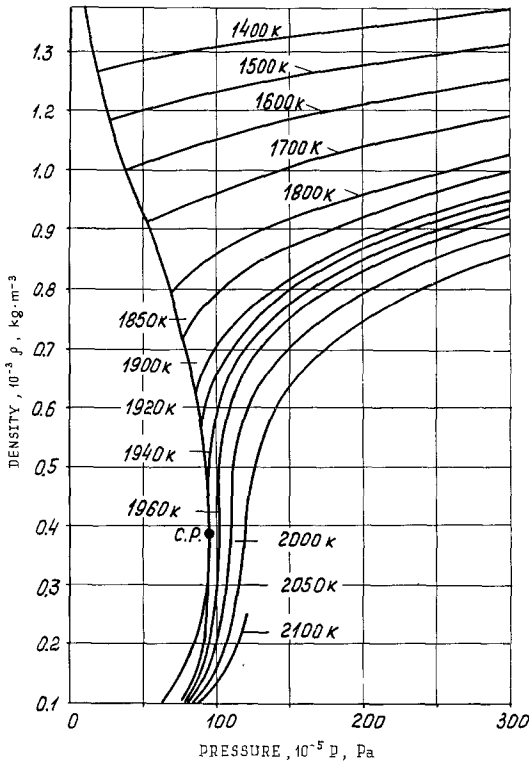
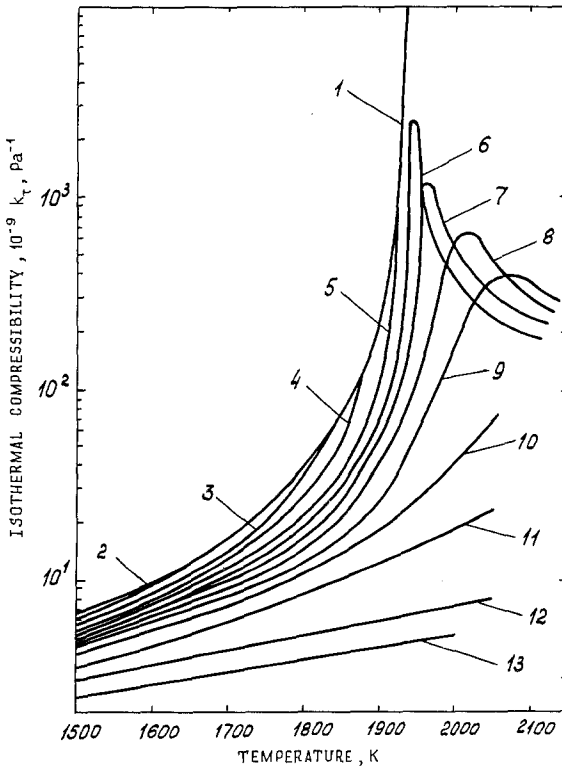


Fig. 2. Cesium equation of state; smoothed data along isotherms.

Usually, this problem is solved by fitting an analytical equation to the experimental data by means of the least-squares method. However, an analytical equation of state for the liquid and dense vapor is not available.

We used a local smoothing method [10] for experimental data treatment. The essence of the method is as follows: a smooth value is obtained as  $\tilde{y}_k = f_k(x)|_{x=x_k}$ , where  $f_k(x)$  are calculated by means of the least-squares technique from the experimental data  $(x_i, y_i)$ , with  $i = k - 2, k - 1, \dots, k + 2$ . The procedure is repeated for  $k = 3, 4, \dots, n - 2$ , where  $n$  is the number of points on the curve. Derivatives were calculated from  $f_k(x)$ :  $\partial f_k / \partial x|_{x=x_k}$  and  $\partial^2 f_k / \partial x^2|_{x=x_k}$ . The experimental points may be smoothed many times. The criterion of sufficiency is the smoothness of the first and second derivatives if the difference between experimental and smoothed data is acceptable.



**Fig. 3.** Isothermal compressibility of cesium. 1, At saturation. Along smoothed isobars: 2, 5 MPa; 3, 7 MPa; 4, 8 MPa; 5, 9 MPa; 6, 9.5 MPa; 7, 10 MPa; 8, 11 MPa; 9, 12 MPa; 10, 15 MPa; 11, 20 MPa; 12, 30 MPa; 13, 60 MPa.

The density  $\rho$ , isothermal compressibility  $k_T = \rho^{-1}(\partial\rho/\partial P)_T$  and thermal expansion  $\alpha_P = -\rho^{-1}(\partial\rho/\partial T)_P$  of cesium for the observed parameters of state are given in Tables I-III and in Figs. 2 and 3.

#### 4. DISCUSSION

As seen from Fig. 1, the coexistence curve of cesium is asymmetric. The reduced density  $|\rho^s - \rho_c|/\rho_c$  versus  $\tau = (T_c - T)/T_c$  ( $\rho^s$ , density at saturation) for the liquid (L) and vapor (V) branches of the coexistence curve are plotted in Fig. 4 (on a logarithmic scale). As is known [11] for dielectric substances, both of the branches are proportional to  $\tau^\beta$  at  $\tau \ll 1$ , where  $\beta = \beta_V = \beta_L \approx 1/3$ . In practice this is true for  $\tau < 10^{-1}$  [12]. As shown in Fig. 4, the situation for cesium is different: for the vapor branch  $\beta_V = 0.34$ , but for the liquid branch  $\beta_L = 0.44$ . The dashed lines are their extrapolation to  $\tau \rightarrow 0$ . In the nearest vicinity of the critical point, both of these dependencies must be  $\beta \approx 1/3$ . According to our data this will be true for cesium at  $\tau < 10^{-3}$ . The observed shape of these plots may be explained, first, by the fact that the metal-insulator transition in cesium takes place in the nearest vicinity of the critical point in agreement with electrical conductivity data for cesium [13], second, that the critical region for cesium is much smaller than for dielectric substances.

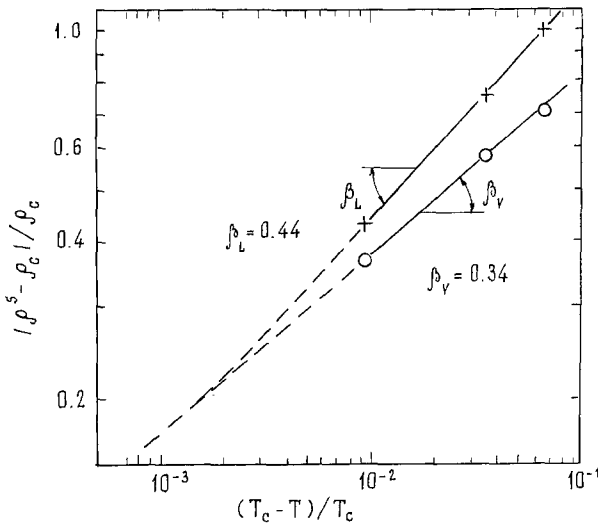


Fig. 4. Liquid and vapor branches of the cesium coexistence curve.



As shown in Fig. 1, the coexistence curve diameter of cesium has a strong curvature. For the first time the violation of "rectilinear-diameter law" was observed for mercury by Kikoin and Senchenkov [14] and then was supported by more precise mercury equation-of-state measurements [15]. Our data on the curvature of cesium coexistence diameter agree with data reported in Ref. 9.

Figure 5 reproduces the Guggenheim plot of the coexistence curves of eight dielectric substances. Coexistence curves of mercury [15] and cesium with their diameters are also shown in Fig. 5. As seen, the principle of corresponding states for mercury and cesium is not observed. This concerns mainly the liquid phase, where the interaction between particles strongly depends on the states of valence electrons. One may assume that the difference of the diameter curvature  $(\rho_L^s + \rho_V^s)/2 = f(T)$  for monovalent cesium and divalent mercury is related to electron spectrum differences in these metals in liquid phase.

The curvature of the diameter for metals may be expected, since the saturation line of metals is in essence the coexistence boundary of two different substance: metallic liquids with strong density dependence of interaction between particles and nonmetal vapor or dense plasma. For mercury

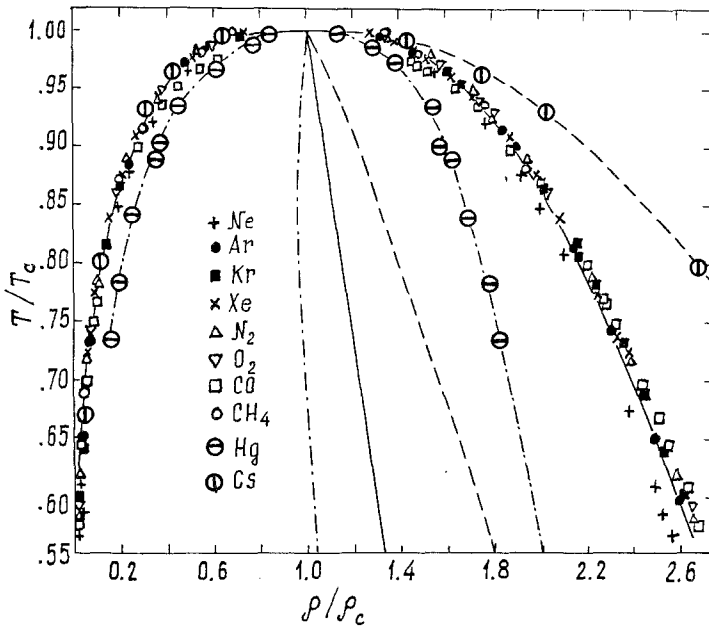


Fig. 5. Coexistence curves and their diameters for dielectric and metallic substances.

the metal–nonmetal transition occurs in the liquid phase at  $\rho \simeq 1.5\rho_c$  [14], which only exaggerates the situation. We believe that the observed curvature of coexistence line diameter is not related to the singularity of the diameter, predicted very close to the critical point.

## REFERENCES

1. N. W. Ashcroft and N. D. Mermin, *Solid State Physics* (Holt, Rinehart and Winston, New York, 1976).
2. R. W. Ohse, J.-F. Babelot, J. Magill, and M. Tetenbaum, in *Handbook of Thermodynamic and Transport Properties of Alkali Metals*, R. W. Ohse, ed. IUPAC, Chem. Data N 30 (Oxford, 1985), pp. 329–347.
3. N. B. Vargaftik, V. F. Kozhevnikov, P. N. Ermilov, and V. A. Alekseev, in *Proc. 8th Symp. Thermophys. Prop.*, Vol. 2, J. V. Sengers, ed. (ASME, New York, 1982), pp. 174–175.
4. N. B. Vargaftik, V. F. Kozhevnikov, and P. N. Ermilov, *High Temp.-High Press.* **16**:233 (1984).
5. V. F. Kozhevnikov and P. N. Ermilov, *Prib. Tekh. Eksp.* **N1**:83 (1982).
6. N. B. Vargaftik, E. B. Gelman, V. F. Kozhevnikov, and S. P. Naurzakov, in *Proc. 11 AIRAPT Int. Conf.*, Vol. 1 (Naukova Dumka, Kiev, 1989), pp. 57–62.
7. N. A. Pokrasin, V. V. Roshchupkin, L. R. Fokin, N. B. and Khandomirova, *Teplofiz. Svoistva Veshchestv Mater.* **19**:33 (1983) (in Russian).
8. N. B. Vargaftik, L. D. Voljak, and V. G. Stepanov, in *Handbook of Thermodynamic and Transport Properties of Alkali Metals*, R. W. Ohse, ed. IUPAC Chem. Data N 30 (Oxford, 1985), pp. 641–666.
9. S. Jungst, B. Knuth, and F. Hensel, *Phys. Rev. Lett.* **55**:2160 (1985).
10. C. Lanczos, *Applied Analysis* (Prentice Hall, Englewood Cliffs, N.J., 1956).
11. E. A. Guggenheim, *J. Chem. Phys.* **12**:253 (1945).
12. P. R. Roach, *Phys. Rev.* **170**:213 (1968).
13. F. Hensel, in *Proc. 8th Symp. Thermophys. Prop.*, Vol. 2, J. V. Sengers, ed. (ASME, New York, 1982), pp. 151–158.
14. I. K. Kikoin and A. P. Senchenkov, *Fiz. Metal. Metalloved.* **24**:843 (1967) (in Russian).
15. I. K. Kikoin, A. P. Senchenkov, S. P. Naurzakov, and E. B. Gelman, Preprint IAE-2310 (Moscow, 1973) (in Russian).